JMEPEG (2012) 21:1160–1166
DOI: 10.1007/s11665-011-0033-y

1059-9495/$19.00

# An Application of ANFIS to Predict the Hot Flow Behavior of 6063 Aluminum Alloy

*Gan Chunlei and Wang Mengjun*

*(Submitted November 27, 2010; in revised form July 19, 2011)*

**In order to determine the optimum hot-forming processing parameters for 6063 aluminum alloy, the compressive deformation behavior of 6063 aluminum alloy was investigated at the temperatures from 300 to 500 °C and strain rates from 0.5 to 50 $s^{-1}$ on a Gleeble-1500 Thermal Simulator. Based on the compression experimental data, a novel adaptive network-based fuzzy inference system (ANFIS) model is developed to predict the flow behavior of 6063 aluminum alloy. In the ANFIS system, the inputs of the ANFIS are the strain, the strain rate and the temperature, whereas the flow stress is the output. The effects of strain, strain rate, and temperature on the flow behavior of 6063 aluminum alloy have been studied by comparing the experimental and the predicted results using the developed ANFIS model. The results show that predicted values using the developed model are in good agreement with the experimental data, which demonstrates the reliability of the developed ANFIS model.**

**Keywords** 6063 aluminum alloy, ANFIS, flow stress

## 1. Introduction

The constitutive flow behaviors of materials during hot-forming processes are greatly complex due to the effects of some metallurgical phenomena, such as work hardening, dynamic recovery, dynamic recrystallization, flow instabilities, and so on. These metallurgical phenomena often make the relationship between flow stress and the process parameters nonlinear. In the past, numerous efforts have been invested in developing constitutive equations on the basis of the regression analysis with the experimental results to represent the flow stress of materials (Ref 1–6). However, the accuracy of the regression method in prediction is relatively low, and the applicable range can be also limited because of the highly nonlinear flow behavior of materials under hot deformation. Therefore, it is necessary to develop some advanced computing methods to further increase the accuracy of prediction.

Recently, adaptive network-based fuzzy inference system (ANFIS) theory has been introduced into describing the hot deformation process (Ref 7). ANFIS is an adaptive network which permits the application of neural network topology together with fuzzy logic (Ref 8). The combination of these two methods provides a better selection to materials' modeling and material processing control techniques than traditional computational methods. ANFIS has been successfully applied in many scientific researches and engineering practices (Ref 9–13). One significant advantage of the ANFIS approach is that it does not need a mathematical formulation for algorithmically converting an input to an output. The mapping relation between the input and output data can be constructed through fast learning to realize optimal parameters of a given fuzzy inference system (FIS). Owing to considerable advantages, such as modeling the uncertainty ability of FISs, learning capability of neural networks, nonlinear ability, capacity for fast learning, and adaptation capability, ANFIS is ideally suited for solving complex and nonlinear deformation behaviors of materials. However, at present there is no report on the application of ANFIS to predict the flow stress of commercially important 6063 aluminum alloy which is extensively used in the structural applications because of its remarkable combination of characteristics in terms of the low density, the high corrosion resistance, high strength, and easy workability.

The main object of the study is to develop an efficient ANFIS model to accurately predict the constitutive flow behavior of 6063 aluminum alloy during hot compression deformation, and the effects of strain, strain rate, and temperature on the compressive deformation characteristics of 6063 aluminum alloy are also investigated.

## 2. Experimental Procedures

In this study, the commercial 6063 aluminum alloy with chemical compositions of 0.423Si-0.043Cu-0.7Mg-0.145Fe-0.002Mn-0.008Ti-0.046Cr, and (bal.) Al (wt.%) was used. The as-received specimen for optical metallography was ground and electropolished using an acidic solution(20 mL $H_2O$, 14 mL $H_2SO_4$, 57 mL $H_3PO_4$, and 9 g $CrO_3$); After being rinsed by water, the specimen was subsequently anodized in another acidic solution (1000 mL $H_2O$, 40 mL HF (solubility 30%),

**Gan Chunlei**, Institute for Advanced Materials and Technologies, University of Science and Technology Beijing, Beijing 100083, People's Republic of China; and Key Laboratory for Advanced Materials Processing (Ministry of Education), University of Science and Technology Beijing, Beijing 100083, People's Republic of China; and **Wang Mengjun**, Key Laboratory of Nonferrous Metal Materials Science and Engineering of Ministry of Education, Central South University, Changsha 410083, People's Republic of China. Contact e-mail: ganchunlei@163.com.

and 11 g $H_3BO_3$). The microstructure was examined using polarized optical microscope. Figure 1 shows that the as-received microstructure of 6063 aluminum alloy consists of equi-axed grains with a size of about 100 μm. The test specimen geometry was a 15-mm-high cylindrical bar with the diameter of 10 mm. The flat ends of the specimen were recessed to a depth of 0.2 mm deep to retain the lubricant of graphite mixed with machine oil during compression tests. The lubricant was used for reducing the effect of friction between the specimen and anvils. A series of compression tests were carried out on a Gleeble-1500 Thermal Simulator in the temperature range of from 300 to 500 °C with the strain rates of 0.5-50 $s^{-1}$. All the specimens were heated up to test temperatures at the rate of 100 °C/min and hold for 3 min to prevent a volumetric change due to thermal expansion before compression. The reduction in height is 50% at the end of the compression tests. True stress–strain curves of 6063 aluminum alloy can be transformed from the load-displacement data which were recorded automatically by the computer control system of the thermal simulator. Figure 2 shows the typical examples of true stress-true strain curves obtained from hot compression tests of 6063 aluminum alloy.

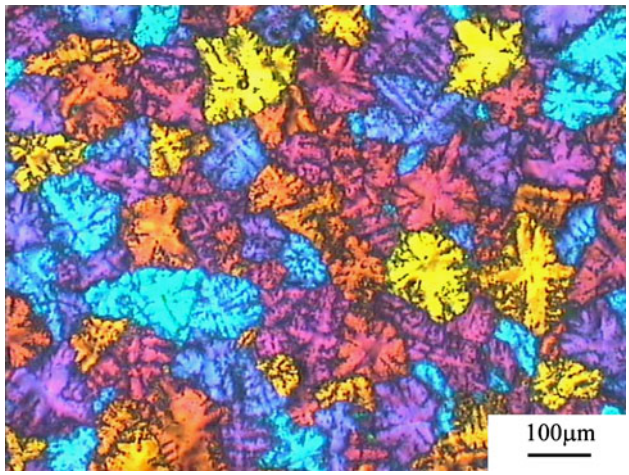


**Fig. 1** The as-received microstructure of 6063 aluminum alloy

## 3. Development of ANFIS for Flow Stress Prediction

### 3.1 Architecture of ANFIS

The ANFIS system is a hybrid method wherein the FISs are combined with neural networks. In the ANFIS system, the FISs are used to compensate for the drawbacks of neural networks which are very difficult to adopt a prior knowledge about the given system. Therefore, ANFIS is functionally equivalent to the combination of neural network and FIS.

The structure of the neuro-fuzzy system was a first-order Sugeno fuzzy model known as an ANFIS (Ref 14). In order to simplify the explanations, the FIS under consideration is assumed to have two inputs ($x$ and $y$) and one output, where its rule is:

Rule 1: If $x$ is $A_1$ and $y$ is $B_1$, then $f_1 = p_1 x + q_1 y + r_1$ (Eq 1)

Rule 2: If $x$ is $A_2$ and $y$ is $B_2$, ; then $f_2 = p_2 x + q_2 y + r_2$ (Eq 2)

where $p_1$, $p_2$, $q_1$, $q_2$, $r_1$, and $r_2$ are linear parameters and $A_1$, $A_2$, $B_1$, and $B_2$ are nonlinear parameters. The ANFIS architecture with two inputs and one output is shown in Fig. 3. The entire ANFIS system which consists of five layers—the fuzzy, product, normalized, de-fuzzy, and total output layers—is simply described as follows. Readers are referred to Jang (Ref 15) for details.

**Layer 1** Every node $i$ in this layer is a square node with a node function.

$$O_{1,i} = \mu_{Ai}(x), \quad i = 1, 2 \tag{Eq 3a}$$

$$O_{1,i} = \mu_{B(i-2)}(y), \quad i = 3, 4 \tag{Eq 3b}$$

where $x$ and $y$ are the inputs to node $i$, and $A_i$ and $B_i$ are linguistic labels for the respective inputs. In other words, $O_{1,i}$ is the membership function of $A_i$ and $B_i$, and in the present study, a Gaussian parameterized membership function is used which obtains a smooth transition between rule and rule:

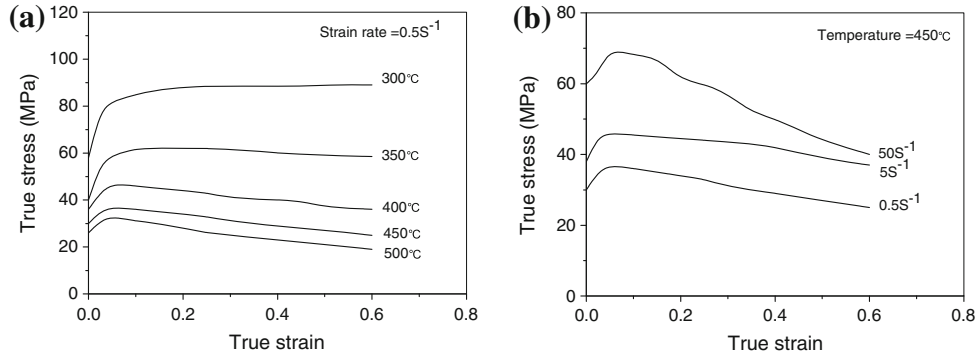


**Fig. 2** Typical true stress–true strain curves for 6063 aluminum alloy under the different deformation temperatures and strain rates

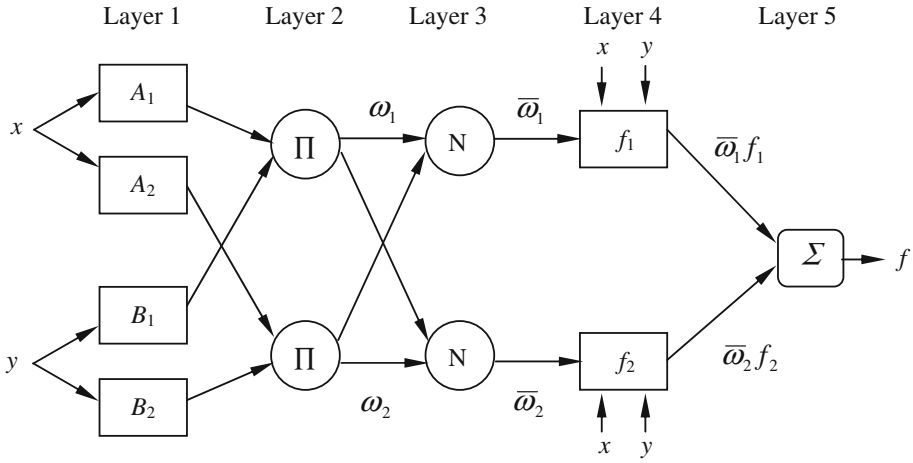


**Fig. 3** ANFIS architecture

$$\mu A(x) = \exp\left\{(-1/2)[(x - c_i)/\sigma_i]^2\right\} \quad \text{(Eq 4)}$$

where ($\sigma_i$, $c_i$) is the parameter set. Nonlinear parameters in this layer are referred to as premise parameters.

**Layer 2** Each node in this layer generates the firing strength of a rule via multiplication by Eq 5.

$$O_{2,i} = \omega_i = \mu_{Ai}(x) \cdot \mu_{Bi}(y), \quad i = 1, 2 \quad \text{(Eq 5)}$$

**Layer 3** The *i*th node calculates the ratio of the *i*th rule's firing strength to the total of all firing strengths by Eq 6.

$$O_{3,i} = \bar{\omega}_i = \frac{\omega_i}{\omega_1 + \omega_2}, \quad i = 1, 2 \quad \text{(Eq 6)}$$

**Layer 4** The *i*th node computes the contribution of the *i*th rule toward the overall output by Eq 7.

$$O_{4,i} = \bar{\omega}_i f_i = \bar{\omega}_i(p_i x + q_i y + r_i), \quad i = 1, 2 \quad \text{(Eq 7)}$$

Linear parameters {$p_i$, $q_i$, and $r_i$} in this layer are referred to as consequent parameters.

**Layer 5** The single node in this layer calculates the overall output as the summation of contributions from each rule. The results can be written as

$$O_{5,i} = \sum_i \bar{\omega}_i f_i = \frac{\sum_i \omega_i f_i}{\sum_i \omega_i}, \quad i = 1, 2 \quad \text{(Eq 8)}$$

### 3.2 Design of ANFIS Model for Flow Stress Prediction

Figure 4 shows the architecture of the ANFIS which consists of 27 fuzzy rules with three Gaussian membership functions being assigned to each input variable. The membership function diagrams of the inputs of the flow stress prediction process before learning can be found in Fig. 5. The inputs of the model are the strain, the temperature and the strain rate. The output of the model is the flow stress. In order to model a given set of input/output data, a hybrid learning algorithm wherein the least squares method is combined with the back-propagation gradient descent method has been used for training the Gaussian membership function parameters. Each epoch of the hybrid learning procedure is composed of a forward pass and a backward pass. First, functional signals go forward till layer 4, and consequent parameters are optimized by the least squares method when premise parameters are fixed. Second, the error rates propagate backward, and the premise parameters are updated by the back-propagation gradient descent method.

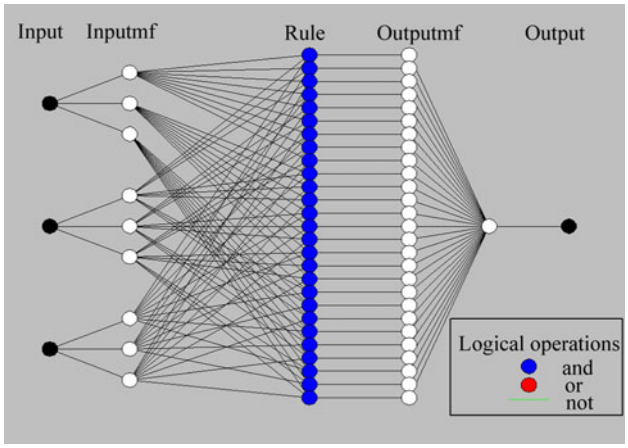


**Fig. 4** Architecture of the ANFIS. Each of the three inputs (true strain, temperature, and strain rate) is connected through its three membership functions to the rule layer. The output values are flow stress

A total of 270 input/output data points from the thermo-simulation compressive experiments were selected from 15 stress–strain curves. Among these datasets, 80% of the datasets were randomly selected to train the ANFIS model, while the remaining 20% were employed to check the predictability of the newly constructed ANFIS system. The initial value of step size for the training was set to 0.01. The flow chart for predicting the flow stress of 6063 aluminum alloy via ANFIS is shown in Fig. 6. The findings are analyzed and discussed in the next section.

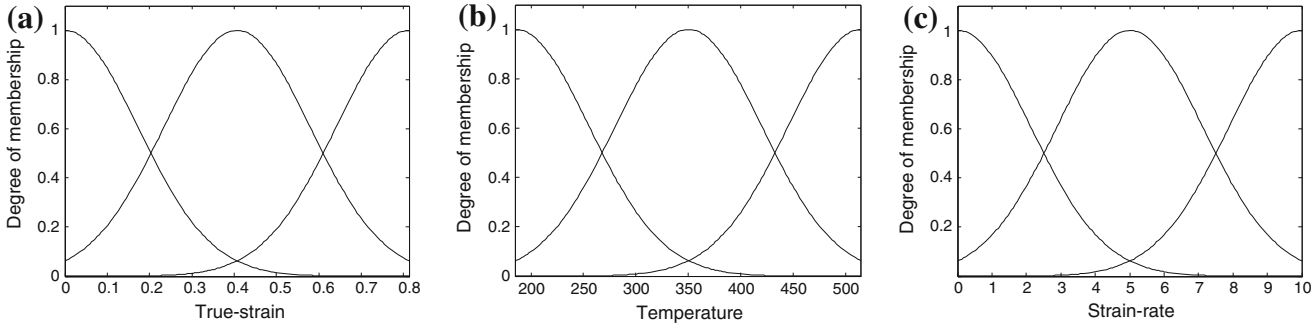


**Fig. 5** The membership function diagrams: (a) true strain, (b) temperature, and (c) strain rate

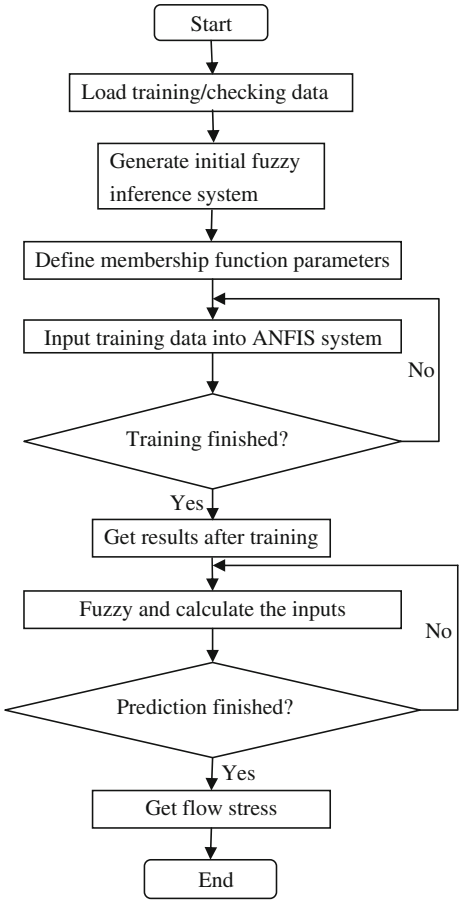


**Fig. 6** Schematic of the ANFIS structure for flow stress prediction for 6063 aluminum alloy

## 4. Results and Discussion

### 4.1 ANFIS Model Performances

The predictability of the developed ANFIS model can be quantified in terms of different measures of prediction error. The error measures include mean percentage error (MPE), root mean square error (RMSE), and correlation coefficient ($R$) defined as follows:

$$\mathrm{MPE} = \frac{\sum_{i=1}^{n} \frac{|p_i - m_i|}{m_i}}{n} \qquad \text{(Eq 9)}$$

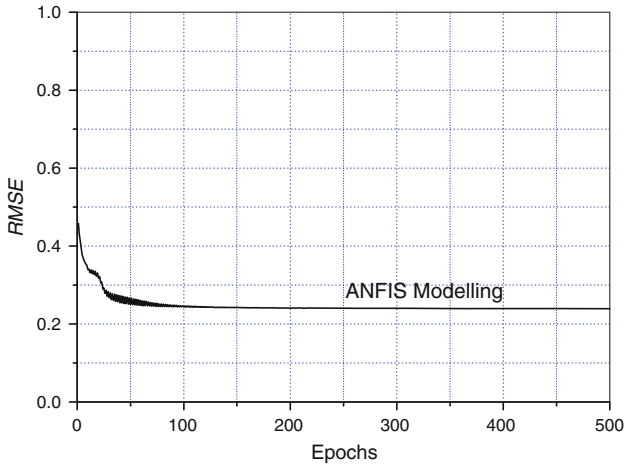


**Fig. 7** Errors on ANFIS modeling

$$\mathrm{RMSE} = \sqrt{\frac{1}{n}\sum_{i=1}^{n}(p_i - m_i)^2} \qquad \text{(Eq 10)}$$

$$R = \frac{\sum_{i=1}^{n}(m_i - \bar{m})(p_i - \bar{p})}{\sqrt{\sum_{i=1}^{n}(m_i - \bar{m})^2 \sum_{i=1}^{n}(p_i - \bar{p})^2}} \qquad \text{(Eq 11)}$$

where $m_i$ is the value of the experimental data, $p_i$ the predicted value, and $n$ the number of samples in the dataset. $\bar{m}$ and $\bar{p}$ are the mean values of $m$ and $p$, respectively. In this study, the performance of the ANFIS model predictions is the value of MPE is only 0.79%; the value of RMSE is 0.5823; and the value of correlation coefficient ($R$) is 0.99948. These prediction errors are considerably satisfactory, which suggests that the ANFIS model can be made applicable for the present study.

Figure 7 shows the RMSE curve for ANFIS modeling. After 500 epochs of training, the root mean square error became steady. Under this circumstance, the training was regarded as converged. This figure displays well how ANFIS can effectively model a flow stress prediction process.

Figure 8 shows the comparison between the experimental and the corresponding predicted results for 6063 aluminum alloy. As indicated, the predicted flow stress is very close to the experimental flow stress. The results show that a good correlation between the experimental and predicted results

has been obtained, which implies that the proposed ANFIS model is able to accurately predict the flow behavior of 6063 aluminum alloy during hot deformation.

### 4.2 Application of the Developed ANFIS Model

The developed ANFIS model can be employed to simulate the effects of temperature and strain rate on the flow behavior of 6063 aluminum alloy. Figure 9 shows the variation of flow stress with different temperatures and strain rates, where the flow stress at a true strain of 0.4 is plotted as a function of the temperature and the strain rate for all tested conditions, respectively. It is apparent that the actual prediction values are in good accordance with the experimental data, and the curvilinear trend of flow stress for all the tested conditions are greatly affected by the temperature and strain rate.

Further, it can be found that the deformation temperature exerts a significant effect on the magnitude of flow stress, as seen in Fig. 9(a). The flow stress of 6063 aluminum alloy decreases with the increase of temperature for all the strain rate levels. It is well known that the dynamic restoration such as recrystallization of the deformed microstructure is controlled by dislocation climb and cross-slip mechanisms (Ref 16). The increase of temperatures decreases the density and multiplication rate of dislocations, and then causes a loss of flow stress. Therefore, it can be seen that the present alloy becomes softer.

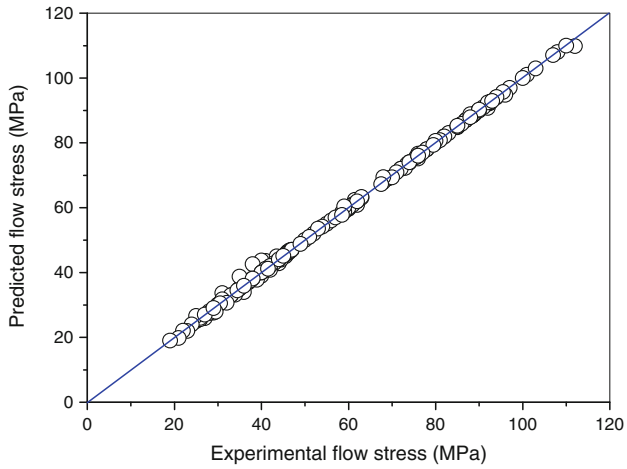


**Fig. 8** Comparison between the experimental and predicted flow stresses of 6063 aluminum alloy using the developed ANFIS model

It can be also found from Fig. 9(a) that the magnitude of flow stress drop varies with the increase of temperature in different temperature and strain rate regions. For all the strain rates, the trend of flow stress drop with increasing temperature at high temperature regions is smaller than that at lower temperature regions. For a given constant strain rate, it is found that a linear relationship is presented over a certain range of temperatures.

The variation of flow stress with strain rate can be clearly seen in Fig. 9(b). The curves indicate that the strain rate has a remarkable effect on the flow stress of 6063 aluminum alloy. As the strain rate increases, flow stress increases because of an increase of dislocation density and the dislocation multiplication rate with strain and strain rate during deformation (Ref 17). However, the ascent magnitude of flow stress with the increase of strain rate is obviously different. For all the temperatures, the ascent magnitude of flow stress with increasing strain rate at high strain rate regions is smaller than that at lower strain rate regions. This can be related to the rapid temperature rise. It should be noted that flow stress is markedly reduced because of the thermal softening when the strain rate is relatively high, for example, 50 $s^{-1}$. It can be explained that heat in the specimen cannot be transferred in good time because the compression deformation is so quick. As a result, the temperature rise of the specimen is rapidly increased. The large temperature rise can further promote flow stress drop.

The effect of strain on the flow behavior of 6063 aluminum alloy is also investigated. Figure 10(a) and (b) shows the comparison between the experimental and predicted flow stresses of 6063 aluminum alloy using the developed ANFIS model under different temperature and strain rate conditions. As shown in Fig. 10, the effect of strain on flow stress is nonsignificant under the lower strain rate and temperature due to the dynamic equilibrium of work hardening and softening; however, the contribution from strain can play an important role when the strain rate is higher and the deformation temperature is increased. It can be found that the marked effect of strain arises mainly from a higher temperature or/and a higher strain rate region where dynamic softening dominates over work hardening. Furthermore, although the strain hardening and flow softening stages are well evidenced, the developed ANFIS model can still predict the trend and level of flow stress.

In order to further evaluate the predictability of the proposed ANFIS model, a 3D surface that takes true strain along the *x*-axis, temperature along the *y*-axis and flow stress along the *z*-axis for 6063 aluminum alloy at a strain rate of 0.5 $s^{-1}$ is given in Fig. 11. The range for true strain and temperature is 0-0.6

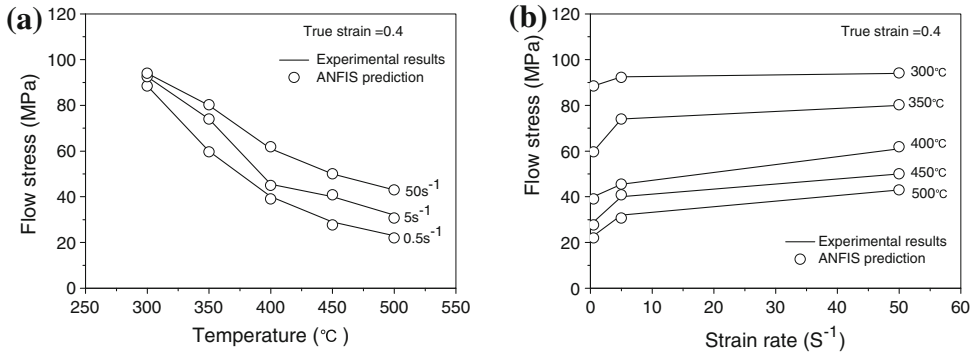


**Fig. 9** Comparison between the experimental and predicted flow stresses of 6063 aluminum alloy using the ANFIS model: (a) effects of the deformation temperatures; (b) effects of the strain rates

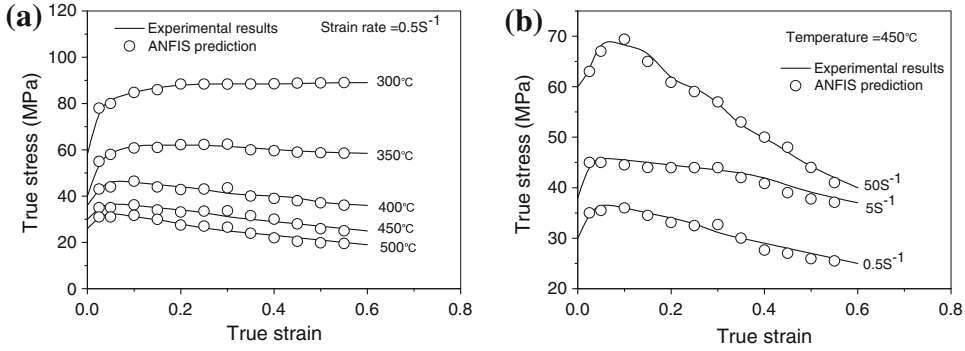


**Fig. 10** Comparison between the experimental and predicted flow stresses of 6063 aluminum alloy using the ANFIS model: (a) strain rate = 0.5 $s^{-1}$; (b) deformation temperature = 450 °C

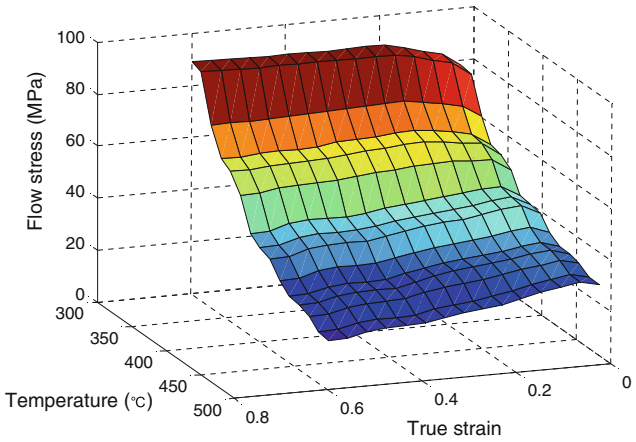


**Fig. 11** ANFIS prediction on relationship of flow stress, versus true strain and temperature at a strain rate of 0.5 $s^{-1}$. There were no experimental data available at this strain rate

and 300-500 °C, respectively. The anticipated variation in flow stress with the deformation temperature and true strain is distinctly plotted in Fig. 11. The ANFIS model's predictions are well in agreement with the experimental results even if experimental data are not available at this strain rate.

## 5. Conclusions

In this study, a novel ANFIS has been developed to predict the constitutive flow behavior of 6063 aluminum alloy using experimental data from hot compression tests at the temperatures from 300 to 500 °C and strain rates from 0.5 to 50 $s^{-1}$. The developed ANFIS model takes the strain, the strain rate, and the temperature as the inputs while the flow stress is the output. The values of MPE and RMSE from the predicted results are 0.79% and 0.5823, respectively, which suggests that the ANFIS model can be made applicable for the present study. By comparing the experimental and the predicted results from the developed ANFIS model, a very good correlation between experimental and predicted results has been obtained even if the strain hardening and flow softening stages are well evidenced. In addition, the results from the ANFIS model and experiments have manifested that strain rate and temperature have great effects on flow stress, whereas the marked effect of strain arises mainly from a higher temperature or/and a higher strain rate regions. It can, therefore, be concluded that the ANFIS model proposed in this article is an efficient quantitative tool to evaluate and predict the flow behavior of 6063 aluminum alloy during hot compression deformation.

## Acknowledgment

The financial supports received for this study from the National Basic Research Program of China (1999064908) and the State Key Laboratory of Material Processing and Die & Mould Technology in Huazhong University of Science and Technology (1999153) are gratefully acknowledged.

## References

1. Z.J. Gronostajski, Constitutive Equations for FEM Analysis, *J. Mater. Process. Technol.*, 2000, **106**, p 40–44
2. S. Mandal, V. Rakesh, P.V. Sivaprasad, S. Venugopal, and K.V. Kasiviswanathan, Constitutive Equations to Predict High Temperature Flow Stress in a Ti-Modified Austenitic Stainless Steel, *Mater. Sci. Eng. A*, 2009, **500**, p 114–121
3. H. Mirzadeh and A. Najafizadeh, Flow Stress Prediction at Hot Working Conditions, *Mater. Sci. Eng. A*, 2010, **527**, p 1160–1164
4. D. Samantaray, S. Mandal, and A.K. Bhaduri, Constitutive Analysis to Predict High-Temperature Flow Stress in Modified 9Cr-1Mo (P91) Steel, *Mater. Des.*, 2010, **31**, p 981–984
5. S.S. Park, H. Garmestani, G.T. Bae, N.J. Kim, P.E. Krajewski, S. Kim, and E.W. Lee, Constitutive Analysis on the Superplastic Deformation of Warm-Rolled 6013 Al Alloy, *Mater. Sci. Eng. A*, 2006, **435-436**, p 687–692
6. S. Spigarelli, M.E. Mehtedi, P. Ricci, and C. Mapelli, Constitutive Equations for Prediction of the Flow Behaviour of Duplex Stainless Steels, *Mater. Sci. Eng. A*, 2010, **527**, p 4218–4228
7. V. Kalaichelvi, D. Sivakumar, R. Karthikeyan, and K. Palanikumar, Prediction of the Flow Stress of 6061Al-15% SiC-MMC Composites Using Adaptive Network Based Fuzzy Inference System, *Mater. Des.*, 2009, **30**, p 1362–1370
8. M. Hayati, A. Rezaei, and M. Seifi, Prediction of the Heat Transfer Rate of a Single Layer Wire-on-Tube Type Heat Exchanger Using ANFIS, *Int. J. Refrig.*, 2009, **32**, p 1914–1917
9. M. Hayati, A. Rezaei, M. Seifi, and A. Naderi, Modeling and Simulation of Combinational CMOS Logic Circuits by ANFIS, *Microelectron. J.*, 2010, **41**, p 381–387
10. S. Zaferanlouei, D. Rostamifard, and S. Setayeshi, Prediction of Critical Heat Flux Using ANFIS, *Ann. Nucl. Energy*, 2010, **37**, p 813–821
11. C.K. Lau, Y.S. Heng, M.A. Hussain, and M.I. Mohamad Nor, Fault Diagnosis of the Polypropylene Production Process (UNIPOL PP) Using ANFIS, *ISA Trans.*, 2010, **49**, p 559–566
12. M. Mehrabi, S.M. Pesteei, and G.T. Pashaee, Modeling of Heat Transfer and Fluid Flow Characteristics of Helicoidal Double-Pipe

Heat Exchangers Using Adaptive Neuro-Fuzzy Inference System (ANFIS), *Int. Commun. Heat Mass Transf.*, 2011, **38**, p 525–532

13. I. Turkmen, Efficient Impulse Noise Detection Method with ANFIS for Accurate Image Restoration, *AEU Int. J. Electron. Commun.*, 2011, **65**, p 132–139
14. T. Takagi and M. Sugeno, Fuzzy Identification of Systems and Its Applications to Modelling and Control, *IEEE Trans. Syst. Man. Cybern.*, 1985, **15**, p 116–132
15. J.-S.R. Jang, ANFIS: Adaptive-Network-Based Fuzzy Inference System, *IEEE Trans. Syst. Man. Cybern.*, 1993, **23**, p 665–684
16. A. Galiyev, R. Kaibyshev, and G. Gottstein, Correlation of Plastic Deformation and Dynamic Recrystallization in Magnesium Alloy ZK60, *Acta Mater.*, 2001, **49**, p 1199–1207
17. W.S. Lee, W.C. Sue, C.F. Lin, and C.J. Wu, Strain Rate and Temperature Dependence of the Dynamic Impact Properties of 7075 Aluminum Alloy, *J. Mater. Process. Technol.*, 2000, **100**, p 116–122